Impact of Flux Barrier Shape and Design Strategy in Synchronous Reluctance Machine Optimisation

Christophe De Gréef[1], Virginie Kluyskens[1], Bruno Dehez[1]*

[1]*Institute of Mechanics, Materials and Civil Engineering (iMMC),*
Université catholique de Louvain (UCLouvain), Louvain-la-Neuve, Belgium
**christophe.degreef@uclouvain.be*

Keywords: JOUKOWSKI, OPTIMISATION, SYNRM, DESIGN, FEM

Abstract

Optimal design of synchronous reluctance machines involves a number of parameters and costly finite element evaluations, leading to an intrinsic high optimisation time. To lower it, both the design space and the design approach can be adapted. In this study, the impact on the total optimisation time and achievable performance of four rotor geometries and two design approaches is investigated. The four geometries of interests are rotors having round or Joukowski flux barriers, with or without cut-off barrier. The first design approach consists in carrying a single optimisation to maximise the mean torque while constraining the torque ripple and the local von mises stresses. The second consists in optimising successively the flux barriers for the magnetic performance with an analytical pre-dimensioning of the radial ribs, and then the ribs for the structural integrity. Results show no significant difference in the mean torque and optimisation time between the geometries when carrying a single optimisation. Also, carrying successive optimisations lead to the same performance. While the total optimisation time is not significantly reduced for round flux barriers with this last approach, it can be divided by up to four when using Joukowski flux barriers, regardless of the presence of a cut-off barrier.

1 Introduction

Reluctance motors have the simplest structure of any electric machine. Because their rotor is only composed of ferromagnetic material, they have reduced manufacturing costs and higher reliability. Moreover, the absence of permanent magnets allows higher operating temperature and breaks free of the long-term availability of rare-earth materials. The initial drawbacks of these machines were a low torque output, linked to a low saliency ratio, and a high torque ripple. In 1923, J. K. Kostko pointed out that, in the case of a salient pole design, widening the cut-off barrier to increase the q-axis inductance would produce an unwanted reduction of the d-axis inductance [1]. For that reason, he analysed a different rotor structure featuring the use of multiple flux barriers for increased performance, which will later become the so-called synchronous reluctance motors (SynRM).

The construction of such rotors can be done in, mainly, two different ways. Either the magnetic laminations can be cut axially, so that they are stacked radially, or they can be cut transversally, so that they are stacked axially. If the former guarantees better electromagnetic performance, it also needs specific tooling for the assembly. For that reason, transversally laminated topology has imposed itself for being in-line with the existing manufacturing processes.

In this topology, the structural integrity of the laminations is ensured by small ribs that link all the flux guides together. These ribs must be as narrow as possible because they act as a q-axis magnetic short circuit that reduces the saliency ratio, and, therefore, the electromagnetic performance, but wide enough to withstand the magneto-mechanical loading the rotor is subjected to. That makes the design of SynRM an inherent multi-physics process.

If topology optimisation seems to be an appropriate tool to obtain the optimal design of the rotor, it is still very challenging to implement efficiently, especially when considering magnetic saturation. Moreover, to the authors' knowledge, there are still no reports of a topology solution having better performance than a solution obtained by the more conventional parametric optimisation.

Because parametric optimisations often involve many parameters and computationally expensive finite-element (FE) models, several strategies are adopted to lower the global optimisation time with a minimal trade-off on the achievable performance. In [2], the impact of several flux barrier shape on the mean torque, torque ripple, and global optimisation time is investigated, without considering the mechanical aspects of the machine. The results show that the best performing shape is the round flux barriers [3]. For half its optimisation time, the Joukowski shape [4], which follows the natural flux lines in a solid rotor, almost outputs the same mean torque and torque ripple.

Instead of playing on the design space, other studies focus on finding alternative design approaches to further lower the global optimisation time, i.e., combining differently the objectives and constraints with subsets of the design space [5-6]. In [7], the quality of the solution and the global optimisation time of various design approaches applied to Joukowski flux barriers have been compared. Results show that the global optimisation time can be significantly lowered by performing a magnetic optimisation followed by a mechanical optimisation, with little impact on the magnetic performance. Pre-dimensioning the radial ribs within the magnetic optimisation, as suggested in [8], benefits both the quality of the solution and the global optimisation time.

Nonetheless, it is still unclear which flux barrier shape performs the best when adding the structural integrity constraint to the design objectives. Indeed, the thicknesses of the ribs directly depend on the mass distribution of the rotor and, therefore, the shape of the flux barriers. This might increase the performance gap round flux barriers have over the Joukowski flux barriers, as round flux barriers are described with twice as many parameters, hence offering a wider design space to fine-tune the mass distribution of the rotor. Moreover, while Joukowski flux barriers benefits from a significant lower optimisation time in [7] due to a smaller design space, this might no-longer be true after adding the many parameters describing the ribs to the design space. Pushing further the analysis on the mass distribution of the rotor, the use of a cut-off barrier, as seen in many studies [9-10], lowers the peripheral mass. Consequently, ribs of rotor having a cut-off barrier are expected to be smaller, which should benefit the magnetic performance.

Therefore, the current study aims at comparing the round flux barriers and Joukoswki flux barriers with and without cut-off barrier, in terms of magnetic performance and total optimisation time. Each geometry is optimised to maximise the mean torque while keeping the torque ripple limited and ensuring the structural integrity of the rotor. Moreover, the validity of the optimal design approach observed in [7] is checked for all the considered rotor geometries. This approach consists in performing a magnetic optimisation of the flux barriers with an analytical pre-dimensioning of the radial ribs, followed by a mechanical optimisation of the ribs.

The contents of this study are structured as following. Section 2 presents the parameters used to describe the rotor geometry, for round and Joukowski flux barriers, with and without cut-off barrier. The finite element (FE) models used for the magnetic and mechanical evaluations are detailed in section 3. Section 4 gives the design objectives and constraints as an optimisation problem and describes the two design approaches applied to solve it. Finally, results are reported in section 5.

2 Parametrisation

For this study, we focused the design on the rotor of a 4 poles motor, with 4 flux barriers per pole and a fixed stator.

The parametrisation of round and Joukowski flux barriers is split in two subsets of parameters, those describing the shape

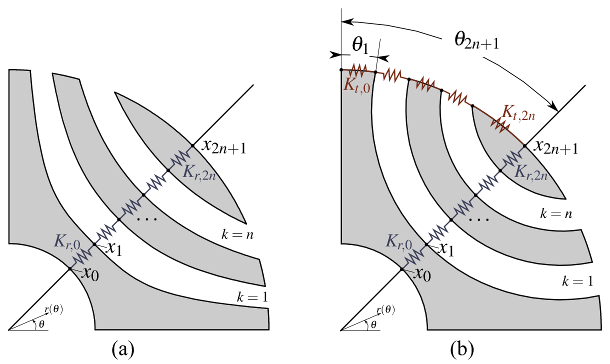

Fig. 1. Parametrisation used to describe n flux barriers without cut-off (a) Joukowski shape. (b) Round shape. For a reason of clarity, only two flux barriers are represented.

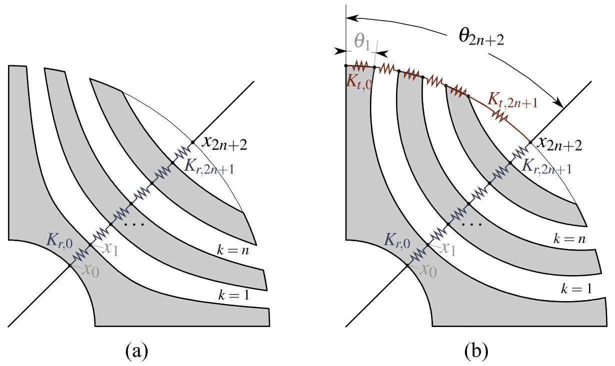

Fig. 2. Parametrisation used to describe n flux barriers with cut-off (a) Joukowski shape. (b) Round shape.

of the flux barriers, $\boldsymbol{x}_{\mathrm{mag}}$, and those describing the ribs, $\boldsymbol{x}_{\mathrm{mec}}$. Each flux barrier is characterised by their inner and outer boundaries. Assuming the rotor to be symmetrical, only the radial position is needed to describe a Joukowski-shaped boundary, whereas a round-shaped boundary requires both its radial position and its opening in the tangential position. This is depicted in Fig. 1.

The Joukowski shape function is given analytically in cylindrical coordinates (r, θ) [4]:

$$r(\theta) = R_{in} \cdot \sqrt{\frac{C+\sqrt{C^2+4\sin^2(p\theta)}}{2\sin(p\theta)}}, \tag{1}$$

with R_{in} the inner radius of the rotor, p the number of pole pairs, and C a constant depending on the radial x position of the curve along the symmetry line of the roto, at $\theta = \pi/2p$:

$$C(x) = \frac{\left(\frac{x}{R_{in}}\right)^{2p} - 1}{\left(\frac{x}{R_{in}}\right)^{p}}. \tag{2}$$

To exclude any possibility of overlap between boundaries of the same flux barriers or of different flux barriers, the radial positions of the boundaries are determined indirectly with a set of virtual springs that repel constructive points that cannot meet [2], as shown in Fig. 1 (a). The radial stiffnesses $K_{r,i}$ are the new design parameters, which yields a parameter space with no other internal constraint than the positiveness of the stiffnesses. The relationship between the position of the i^{th} Joukowski line x_i and the radial stiffness $K_{r,i}$ is:

$$x_i = x_{i-1} + \frac{K_{r,i}}{\sum_{k=0}^{2n} K_{r,k}}(x_{2n+1} - x_0), \tag{3}$$

with $x_0 = R_{in}$ and $x_{2n+1} = R_{ext}$. In this equation, n is the number of flux barriers and R_{ext} the outer radius of the rotor.

For round flux barriers, the openings of the boundaries are determined by another set of virtual springs, Fig. 1 (b). In this case, the relationship between the opening angle θ_i and the tangential stiffness $K_{t,i}$ is:

$$\theta_i = \theta_{i-1} + \frac{K_{t,i}}{\sum_{k=0}^{2n} K_{t,k}}(\theta_{2n+1} - \theta_0), \tag{4}$$

with θ_0 = 0 and $\theta_{2n+1} = \pi/2p$.

Adding the cut-off barrier to these geometries simply consists in adding an extra boundary shape at the periphery of the rotor

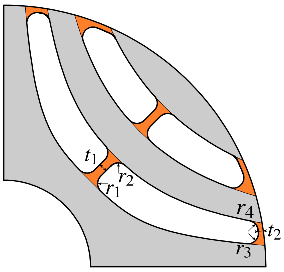

Fig. 3. Parametrisation used to describe radial and tangential ribs.

(Fig. 2). This adds 1 parameter in the case of a Joukowski shape, and 2 parameters in the case of a round shape.

Finally, radial and tangential ribs ensure the structural integrity of the rotor. Each of them is parametrised by a thickness t and circular fillets of radius r, as shown in Fig. 3.
Accounting for the ribs adds 6 parameters per flux barrier to the design space, regardless of the shape of the flux barriers and the presence of cut-off barrier.

3 Magnetic and mechanical evaluations

The electromagnetic performance of the machine is evaluated using a 2D quasi-static FE model. The nonlinear $B-H$ characteristic of the magnetic material is accounted for by using an iterative Newton-Raphson resolution scheme. The torque is obtained through the integration of the Maxwell stress tensor in the airgap. Simulations are carried out at 150 different rotor positions over a pole to properly capture the torque ripple. The synchronous operation of the motor is simulated by prescribing the phase of the sinusoidal currents in coherence with the position increments. The model profits from the periodicity of the problem to lower the number of degrees of freedom (DoF). The resolution time is further reduced by using the moving band method. With this method, the rotor and stator geometry are meshed once, and the position increment simply consists in rotating the rotor mesh. Triangular mesh elements are then inserted in the middle of the airgap to stitch the stator mesh with the rotor mesh. Because the meaning of each DoF is kept the same, the result of the previous position can directly be used as starting point of the new nonlinear resolution. That drastically lowers the iterations needed in the Newton-Raphson resolution scheme, which benefits the global resolution time.
The mechanical stresses are obtained by another 2D FE model. The linear elasticity equations are solved on the rotor geometry, which is subjected to centrifugal effects. The magnetic loading is neglected.
Both these models use the mesh generator Gmsh [10] and the solver GetDP [11]. A fine discretization is used to keep the results as accurate as possible. An example of the meshes used during the optimisation is shown in Fig. 4.

4 Design

Optimal design of SynRMs aims at finding the rotor geometry that maximises the mean torque while constraining the relative

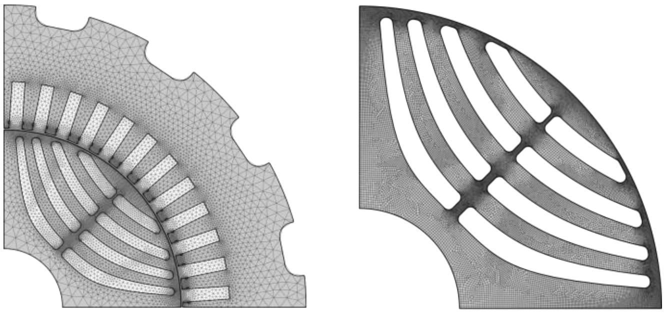

(a) (b)

Fig. 4. Example of meshes used to perform FE simulations. (a) Magnetic mesh (rotor + stator), that has around 28000 triangular elements. (b) Mechanical mesh (rotor only), that has around 35000 rectangular elements.

Table 1 Design space boundaries ($i=0,1,\dots,2n$), ($k=1,2,\dots,n$). Adding the cut-off barrier adds an extra spring to each stiffness network. Round flux barriers have an extra stiffness network.

Param.	Usage	Lower bound	Upper bound	Unit
$K_{r,i}$	All geometries	1	10	–
$K_{r,2n+1}$	If cut-off (round or Joukowski)	1	10	–
$K_{t,i}$	Round only	1	10	–
$K_{t,2n+1}$	If cut-off (round only)	1	10	–
$r_{1,k}$	All geometries	1	10	mm
$r_{2,k}$	All geometries	1	10	mm
$t_{r,k}$	All geometries	0	5	mm
$r_{3,k}$	All geometries	1	10	mm
$r_{4,k}$	All geometries	1	10	mm
$t_{t,k}$	All geometries	0.3	8	mm

torque ripple to 10% and the local von Mises stresses under 270 MPa, with the design space boundaries given in Table 1. The top of this table corresponds to the magnetic parameters $\boldsymbol{x}_{\text{mag}}$, and the bottom to the mechanical parameters $\boldsymbol{x}_{\text{mec}}$. Formally, this optimisation problem is written:

$$\begin{aligned} &\max_{\boldsymbol{x}_{\text{mag}},\boldsymbol{x}_{\text{mec}}} \ \bar{T}(\boldsymbol{x}_{\text{mag}},\boldsymbol{x}_{\text{mec}}) \\ \text{s.t.}\quad &\max(\sigma_{VM}) < 270\ \text{MPa} \\ &T(\boldsymbol{x}_{\text{mag}},\boldsymbol{x}_{\text{mec}}) < 10\%\,. \end{aligned} \tag{5}$$

Two different approaches will be applied to solve the optimisation problem (5), as shown in Fig. 5.

1. The first approach consists in applying the optimisation problem as it is. A high optimisation time is expected due to the large number of parameters. Nonetheless, this approach is expected to find the best solution.

2. The second approach consists in carrying a magnetic optimisation followed by a mechanical optimisation on subsets of the initial design space. As suggested in [7], this is expected to lower the total optimisation time with a limited trade-off on

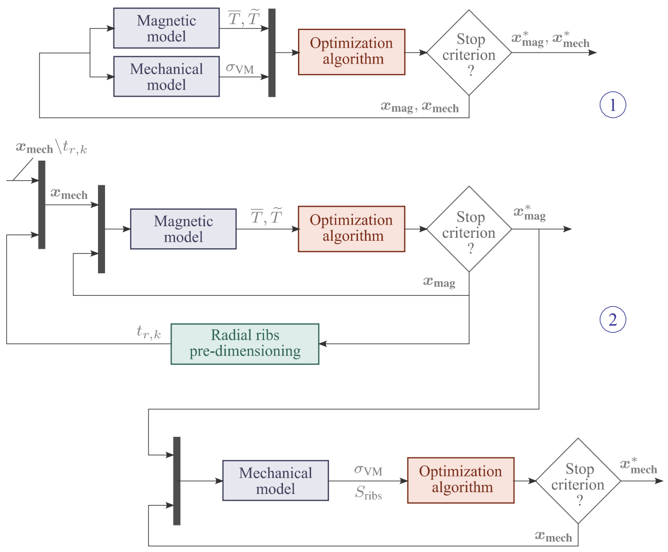

Fig. 5. Approaches to deal with the initial optimisation problem. (1) The optimisation is applied as it is, (2) The optimisation is split in two.

the magnetic performances. Nonetheless, a violation of the torque ripple constraint might occur.

The magnetic optimisation aims at finding the flux barriers parameters $\boldsymbol{x}_{\mathrm{mag}}$ that maximise the mean torque under the torque ripple constraint.

$$\begin{aligned} &\max_{\boldsymbol{x}_{\mathrm{mag}}} \overline{T}(\boldsymbol{x}_{\mathrm{mag}})|_{\boldsymbol{x}_{\mathrm{mec}}} \\ \text{s. t.} \quad &\widetilde{T}(\boldsymbol{x}_{\mathrm{mag}})|_{\boldsymbol{x}_{\mathrm{mec}}} < 10\%. \end{aligned} \tag{6}$$

An analytical pre-dimensioning of the radial ribs is performed within this optimisation, as suggested in [8].

The mechanical optimisation that follows aims at finding the ribs parameters $\boldsymbol{x}_{\mathrm{mec}}$ that minimise the cumulative rib surface S_{ribs} under the local von Mises stresses constraint:

$$\begin{aligned} &\min_{\boldsymbol{x}_{\mathrm{mec}}} \; S_{\mathrm{ribs}}(\boldsymbol{x}_{\mathrm{mec}})|_{\boldsymbol{x}^*_{\mathrm{mag}}} \\ \text{s. t.} \quad &\max(\sigma_{VM}) < 270 \text{ MPa}. \end{aligned} \tag{7}$$

Iterating on the second approach is expecting to compensate for the ignored cross-coupling between the mechanical parameters and the magnetic objectives. The iteration consists in injecting the newly optimised $\boldsymbol{x}^*_{\mathrm{mag}}$ and $\boldsymbol{x}^*_{\mathrm{mec}}$ as initial guess of the approach.

Table 2 Normalised mean torque and total optimisation time obtained after applying approach 1 on the geometries.

	Mean Torque (p.u.)	**Total optimisation time (p.u.)**
Joukowski	1	1
Joukowski (cut-off barrier)	0.995	0.792
Round	1.006	0.806
Round (cut-off barrier)	1.002	1.134

5 Results

The mean torque and total optimisation time obtained by carrying a single optimisation, approach 1, are reported in Table 2. The values are normalised by the results of the Joukowski shape without cut-off barrier, which outputs 1250 Nm and took 302 hours to optimise using the Intel i9-7940X CPU (14 cores, 4.3 GHz). The torque ripple is not shown in this table as this design approach explicitly accounts for the torque ripple constraint which leads, for all the designs, to a relative torque ripple of almost exactly **10**%. According to these results, no flux barrier shape leads to significant better torque, which is coherent to the observations performed in [7]. Moreover, the presence of a cut-off barrier has a negligible impact on the magnetic performances. There is no significant difference in the total optimisation time between Joukowski and round flux barriers, contrarily of the observations in [2]. This is due to a design space having a similar size for the different geometries when accounting for the parameters linked to the ribs, $\boldsymbol{x}_{\mathrm{mec}}$. Indeed, this study case involves 34 parameters for Joukowski flux barriers and 43 parameters for round flux barriers, without cut-off.

The results obtained by design approach 2 are presented in Table 3. The observations performed in [7] remain valid for the considered rotor geometries. Approach 2 can efficiently reduce the total optimisation time with a limited impact on the achievable mean torque. Nonetheless, Joukowski flux barriers benefit more from this design approach than round flux barriers. This arises from the significantly smaller subset of parameters $\boldsymbol{x}_{\mathrm{mag}}$ that are optimised through a costly magnetic optimisation, involving 10 parameters for Joukowski flux barriers instead of 19 parameters for round flux barriers. Iterating on approach 2 brings the mean torque very close to the ones of approach 1, as shown by Table 4. The torque ripple is also diminished, except for the round flux barriers without cut-off. The total optimisation time after iterating is still interesting for Joukowski flux barriers, with half the optimisation time of the single optimisation approach.

Table 3 Normalised mean torque and total optimisation time obtained after applying approach 2 on the geometries.

	Mean Torque (p.u.)	**Torque Ripple (p.u.)**	**Total optimisation time (p.u.)**
Joukowski	0.983	1.597	0.166
Jouko. (cut-off)	0.996	1.302	0.225
Round	0.996	0.915	0.556
Round (cut-off)	1.000	2.313	0.970

Table 4 Normalised mean torque and total optimisation time obtained after iterating on approach 2.

	Mean Torque (p.u.)	**Torque Ripple (p.u.)**	**Total optimisation time (p.u.)**
Joukowski	0.999	0.668	0.459
Jouko. (cut-off)	0.995	0.825	0.557
Round	1.005	2.051	0.966
Round (cut-off)	1.001	1.027	1.511

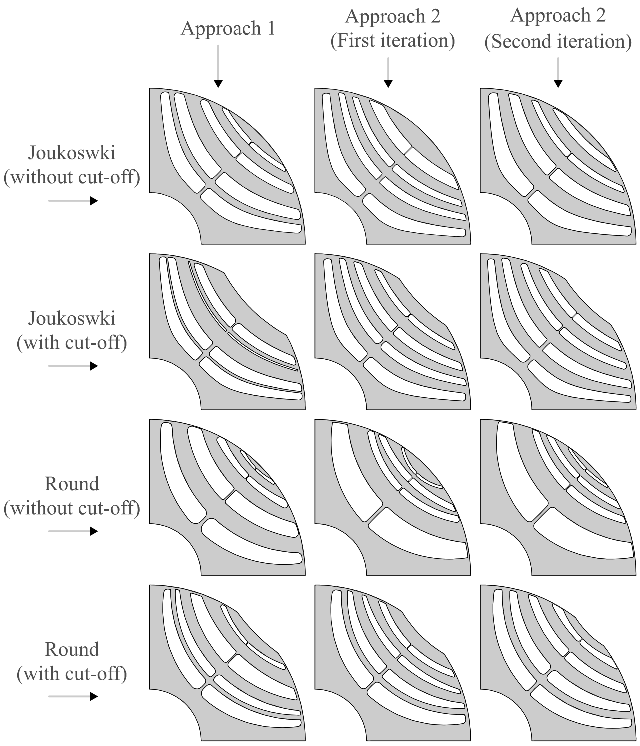

Fig. 6. Optimised geometries.

The geometries obtained at the end of design approaches 1 and 2 are shown in Fig. 6.

6 Conclusion

Two different design approaches are applied on four different rotor geometries to ensure high mean torque, low torque ripple, and structural integrity. The considered geometries have Joukowski or round flux barriers, with or without cut-off. Results show that all these geometries lead to similar performance and total optimisation time when carrying a single optimisation on all the design space. The total optimisation time can be significantly reduced for Joukowski flux barriers by applying the second design approach, which consists in optimising the position and thicknesses of the flux barriers separately from the fillets and thicknesses of the ribs. Round flux barriers benefit less from this approach due to their significantly larger design space describing the position and thicknesses of the flux barriers.

7 References

[1] J. K. Kostko, "Polyphase reaction synchronous motors," in *Journal of the American Institute of Electrical Engineers*.

[2] C. D. Gréef, V. Kluyskens, F. Henrotte, C. Geuzaine and B. Dehez, "Impact of Flux Barriers Shape in Synchronous Reluctance Machine Optimization," *2019 19th International Symposium on Electromagnetic Fields in Mechatronics, Electrical and Electronic Engineering (ISEF)*, 2019.

[3] A. Tessarolo, "Modeling and Analysis of Synchronous Reluctance Machines With Circular Flux Barriers Through Conformal Mapping," in *IEEE Transactions on Magnetics*.

[4] Palmieri, Marco et al. "Effect of the numbers of slots and barriers on the optimal design of synchronous reluctance machines." .

[5] Lopez-Torres, C., Garcia, A., Riba, J.-R., Lux, G., and Romeral, L., "Computationally Efficient Design and Optimization Approach of PMa-SynRM in Frequent Operating Torque-Speed Range".

[6] G. Pellegrino, F. Cupertino and C. Gerada, "Automatic Design of Synchronous Reluctance Motors Focusing on Barrier Shape Optimization,".

[7] C. D. Gréef, V. Kluyskens, F. Henrotte, C. Versèle, C. Geuzaine and B. Dehez, "Time-Efficient Multi-Physics Optimization Approaches for the Design of Synchronous Reluctance Motors, "*13th Annual Energy Conversion Congress and Exposition (ECCE)"*, 2021.

[8] C. Babetto, G. Bacco and N. Bianchi, "Synchronous Reluctance Machine Optimization for High-Speed Applications," in *IEEE Transactions on Energy Conversion*.

[9] W. Doorsamy, M. Muteba, B. Twala and D. V. Nicolae, "Investigation into effects of a novel rotor cut-off design for synchronous reluctance machines,".

[10] I. P. Abeyrathne, M. S. Toulabi and S. Filizadeh, "Design Optimization and Performance Prediction of Synchronous Reluctance Motors," *2018 21st International Conference on Electrical Machines and Systems (ICEMS)*, 2018, pp. 576-581, doi: 10.23919/ICEMS.2018.8548975.

[11] C. Geuzaine and J.-F. Remacle, "Gmsh: A 3-d finite element mesh generator with built-in pre- and post-processing facilities," *International Journal for Numerical Methods in Engineering*, vol. 79, pp. 1309 –1331, 09 2009.

[12] P. Dular, C. Geuzaine, F. Henrotte, and W. Legros, "A general environment for the treatment of discrete problems and its application to the finite element method," in *IEEE Transactions on Magnetics*, vol. 34, no. 5, pp. 3395–3398, Sep. 1998.